Temporal resolution measurement of 128-slice dual source and 320-row area detector computed tomography scanners in helical acquisition mode using the impulse method

Temporal resolution measurement of 128-slice dual source and 320-row area detector computed tomography scanners in helical acquisition mode using the impulse method

Takanori Hara (corresponding author)
Department of Medical Technology, Nakatsugawa Municipal General Hospital, 1522-1 Komanba, Nakatsugawa, Gifu 508-0011, Japan
Email Address: hara_tnk2@ybb.ne.jp
Phone No: +81-573-66-1251(Exi) 2124 Fax No: +81-573-65-6445

Atsushi Urikura
Department of Diagnostic Radiology, Shizuoka Cancer Centre, 1007 Shimonagakubo, Nagaizumi, Sunto, Shizuoka 411-8777, Japan
Email Address: at.urikura@scchr.jp
Phone No: +81-55-989-5222

Katsuhiro Ichikawa
Institute of Medical, Pharmaceutical and Health Sciences, Kanazawa University, 5-11-80 Kodatsuno, Kanazawa, Ishikawa 920-0942, Japan
Email Address: ichikawa@mhs.mp.kanazawa-u.ac.jp
Phone No: +81-76-265-2528

Takashi Hoshino
Department of Radiology, Ishinkai Yao General Hospital, 1-41 Numa, Yao, Osaka 581-0036, Japan
Email Address: hoshi0311@hera.eonet.ne.jp
Phone No: +81-72-948-2500

Eiji Nishimaru
Department of Radiology, Hiroshima University Hospital, 1-2-3 Kasumi, Minami-ku, Hiroshima 734-8551, Japan
Email Address: eiji2403@tk9.so-net.ne.jp
Phone No: +81-82-257-5555

Shinji Niwa
Department of Medical Technology, Nakatsugawa Municipal General Hospital, 1522-1 Komanba, Nakatsugawa, Gifu 508-0011, Japan
Email Address: shinji-niwa.gifu@aria.ocn.ne.jp
Phone No: +81-573-66-1251(Exi) 2124

Abstract

Purpose: To analyse the temporal resolution (TR) of modern computed tomography (CT) scanners using the impulse method, and assess the actual maximum TR at respective helical acquisition modes.

Methods: To assess the actual TR of helical acquisition modes of a 128-slice dual source CT (DSCT) scanner and a 320-row area detector CT (ADCT) scanner, we assessed the TRs of various acquisition combinations of a pitch factor (*P*) and gantry rotation time (*R*).

Results: The TR of the helical acquisition modes for the 128-slice DSCT scanner continuously improved with a shorter gantry rotation time and greater pitch factor. However, for the 320-row ADCT scanner, the TR with a pitch factor of <1.0 was almost equal to the gantry rotation time, whereas with pitch factor of >1.0, it was approximately one half of the gantry rotation time. The maximum TR values of single- and dual-source helical acquisition modes for the 128-slice DSCT scanner were 0.138 (*R*/*P* = 0.285/1.5) and 0.074 s (*R*/*P* = 0.285/3.2), and the

maximum TR values of the 64 × 0.5- and 160 × 0.5-mm detector configurations of the helical acquisition modes for the 320-row ADCT scanner were 0.120 (*R*/*P* = 0.275/1.375) and 0.195 s (*R*/*P* = 0.3/0.6), respectively.
Conclusion: Because the TR of a CT scanner is not accurately depicted in the specifications of the individual scanner, appropriate acquisition conditions should be determined based on the actual TR measurement.

Key words: temporal resolution; helical acquisition mode; gantry rotation time; pitch factor.

Introduction

The temporal resolution (TR) of computed tomography (CT) is an index of a temporal element in a slice image that represents the temporal extent of the contribution of projection data in a reconstructed image. Thus, the TR in the non-helical acquisition (step-and-shoot acquisition) mode with complete projection data per one gantry rotation is equal to the gantry rotation time [1]. In contrast, the TR of the helical acquisition mode to which image reconstruction is performed from z-axis interpolation is closely related to the gantry rotation time and specific interpolation method applied [2]. Thus, because CT images are reconstructed from projection data corresponding to each detector and complex interpolation algorithms [2–4], the TR of the helical acquisition mode may not necessarily be equal to the gantry rotation time of a multi-detector CT [5].

Generally, the TR of conventional helical acquisition modes except the cardiac mode of a CT scanner is not accurately depicted in the specifications of the individual scanner [6, 7]. Therefore, because the TR of a CT scanner is dependent on not only the gantry rotation time but also interpolation algorithms, it should be clarified by an actual measurement.

Taguchi et al. [8] reported that temporal resolution can be evaluated using a temporal sensitivity profile (TSP), defined as the temporal sensitivity distribution of the projection data in a reconstructed CT image, just as the longitudinal spatial resolution can be evaluated by the section sensitivity profile [9, 10]. The TR is determined according to the full width at half maximum (FWHM) of the TSP. Taguchi et al. present the measurement results of the TRs for various reconstruction algorithms by incorporating the implanted temporal impulse signal into the projection data on computer simulations. Thus, if a temporal impulse signal into the reconstructed image (projection data) of commercial CT scanners can be generated by any method, assessment of the actual TR for all acquisition conditions is possible by TSP analysis. In response to this problem, we previously proposed a practical method to assess the TSP of all acquisition modes using an impulse theorem-based metrology (impulse method) [11].

In the present study, we analysed the TR and TSP shape of a modern CT scanner, such as a dual source CT (DSCT) scanner [12] and an area detector CT (ADCT) scanner [13] using the impulse method and assessed the actual maximum TR for particular helical acquisition modes.

Materials and methods

CT scanners

This study was performed using a 128-slice DSCT scanner (SOMATOM Definition Flash; Siemens Healthcare, Erlangen, Germany) and a 320-row ADCT scanner (Aquilion ONE ViSION Edition; Toshiba Medical Systems, Tokyo, Japan). The DSCT scanner is equipped with two X-ray tubes and two 64-row detector arrays mounted into the gantry with an angular offset of approximately 90°. The ADCT scanner is equipped with 320-row detector arrays that can obtain coverage of up to 160 mm in the z-direction. Image data obtained using the two CT scanners were transferred to a dedicated computer using the Digital Image and Communication in Medicine transfer protocol (DICOM) and were analysed using ImageJ image analysis software (ver. 1.47i; National Institutes of Health, Bethesda, MD, USA) [14].

Measurement principle of the impulse method

In our previous report [11], we proposed a practical method to measure the TR using the impulse method, in which a temporal impulse signal is generated by a small metal ball passing through a gantry rotation plane at a very high speed during the respective scan. The passage of the

small metal ball can generate a temporal impulse signal into the projection data. The TR is defined by the TSP, obtained from the various reconstructed impulse response images with very short time increments along the temporal axis. This method can reportedly assess the TR more easily than other methods [15, 16] and can measure not only the TR but also the precise TSP shape. In this impulse method, a streak artefact in a reconstructed CT image is caused by the appearance of the small metal ball on the reconstructed image and the intensity of the streak artefact corresponds to the impulse responses in the temporal domain. Because a patient table (reconstruction) increment can be dealt with as a time increment, the TSP can be obtained from the relationship between the time and region of interest (ROI) values on the streak images. The table position (z) can be converted to time (t) to determine the TSP (t) using the following formula:

$$t = \frac{(z - z_0)R}{WP}$$

R is the gantry rotation time, W is the detector full width and P is the pitch factor (defined as the ratio of the table feed per gantry rotation to the X-ray beam width). The image reconstruction increment should be set to a sufficiently small value such that the corresponding time increment of the TSP data is short enough to accurately detect the TSP shape.

Measurement of TR and TSP

Fig. 1a shows the experimental setup for the impulse method. A small metal ball with an 11-mm diameter was used as the impulse signal and it was shot at high speed along the perpendicular axis at the centre of the gantry rotation plane from the dedicated launching platform by a spring. To verify the speed of the small metal ball, we measured its approximate average velocity using a general digital video camera recording at 120 frames/s in slow motion video mode and a free multimedia player (QuickTime Player 7.7.6; Apple Computers) in a preliminary experiment.

The TR and TSP shape were assessed in a single source helical acquisition mode (SHM) and a dual source helical acquisition mode (DHM) for the 128-slice DSCT scanner; a 64 × 0.5-mm detector configuration in the helical acquisition mode (64HM) and a 160 × 0.5-mm detector configuration in the helical acquisition mode (160HM) for the 320-row ADCT scanner. The acquisition and reconstruction conditions for both CT scanners are presented in Table 1.

The TSPs were obtained from a rectangular 100 × 30-pixel (DHM: 30× 30-pixel) ROI, which was set at the centre of the impulse responses in the respective reconstructed images. We assessed the FWHM as an index value of the TR of the TSP and reported the typical TSPs of various helical acquisition modes of the respective CT scanners.

Results

The average velocity of the small metal ball of 10 consecutive measurements was 11.6 ± 0.3 m/s (mean ± standard deviation) in a preliminary experiment.

Fig. 1b shows reconstructed images from the 128-slice DSCT and 320-row ADCT scanners. The impulse signal of the respective acquisition modes (SHM and DHM) for the 128-slice DSCT appeared as one- and two-streak responses. On the other hand, the 320-row ADCT image appeared as only a one-streak response in the respective reconstructed CT image.

The measured TSPs of the DSCT scanner, which assumed complicated shapes, such as a mixture of triangles and trapezoids, are shown in Fig. 2a and 2b. These shapes were related to the pitch factor in the helical acquisition mode. The measured TSPs of the 320-row ADCT scanner are shown in Fig. 2c and 2d. The TSPs assumed ragged triangular shapes; this ragged frequency was correlated to the pitch factor and detector configuration.

The analytical results of TRs for the 128-slice DSCT scanner as a function of the pitch factor and gantry rotation time are shown in Fig. 3a and 3b, respectively. TRs were proportionally changed according to the pitch factor and gantry rotation time and improved with a larger pitch factor and shorter gantry rotation time. TRs for a pitch factor of 0.5, 0.75, 1.0, 1.25, and 1.5 were approximately 1.8, 1.1, 0.8, 0.6, and 0.5

times the gantry rotation time, respectively, under the respective acquisition conditions. TR for a pitch factor in the vicinity of 0.85 for SHM was approximately equal to the gantry rotation time. The maximum TR values of SHM and DHM were 0.138 (R = 0.285 s; P = 1.5) and 0.074 s (R = 0.285 s; P = 3.2) and the minimum TR values were 0.893 (R = 0.5 s; P = 0.5) and 0.162 s (R = 0.285 s; P = 1.55), respectively. TRs for the 320-row ADCT scanner as a function of the pitch factor and gantry rotation time are shown in Fig. 3c and 3d. TR improved with a larger pitch factor and shorter gantry rotation time. TR for 64HM below a pitch factor of 1.0 was almost equal to the gantry rotation time, while a pitch factor of >1.0 was approximately one half of the value of the gantry rotation time, but it did not continuously change, as observed for the TR of the 128-slice DSCT scanner. The maximum TR values of 64HM and 160HM were 0.120 (R = 0.275 s; P = 1.375) and 0.195 s (R = 0.3 s; P = 0.6), and the minimum TR values were approximately 0.48 (R = 0.5 s; P < 1.0) and 0.314 s (R = 0.5 s; P = 0.569), respectively.

Discussion

The shorter gantry rotation time of the modern CT scanners improved the TR and markedly reduced the likelihood of motion artefacts from physiological movements of the heart, lungs and bowel. However, since the TR of the helical acquisition mode is dependent on not only gantry rotation time but also z-axis interpolation algorithm, an improvement of only the gantry rotation time is insufficient to reduce motion artefacts in CT images. Therefore, TR assessment of the helical acquisition modes for an individual CT scanner is very important to optimize the diagnostic images for the respective purposes.

The results of this study clearly showed that modern CT scanners have remarkable differences in the TR properties in the helical acquisition mode. The TRs for the 128-slice DSCT scanner were relative to the pitch factor and the gantry rotation time and were improved proportionately with larger pitch factor and the shorter gantry rotation time. In addition, the TR value of a pitch factor in the vicinity of 0.85 for SHM was approximately equal to the nominal gantry rotation time. The maximum and minimum TR values of the SHM were 0.138 s (R = 0.285 s; P = 1.5) and 0.893 s (R = 0.5 s; P = 0.5), respectively.

Flohr et al. [12] reported a theoretical TR value for the DHM at a high pitch factor of 3.2 for a 128-slice DSCT scanner. Our measurements indicated that the maximum TR value of the DHM was 0.074 s (R = 0.285 s; P = 3.2). Since the measured TR value almost coincided with the theoretical TR value (0.075 s), this practical measurement method, which uses a small metal ball, is sufficient to obtain accurate TR values under various helical acquisition conditions.

For the 320-row ADCT scanner, the maximum TR values of 64HM and 160HM were 0.120 s (R = 0.275 s; P = 1.375) and 0.195 s (R = 0.3 s; P = 0.6), respectively. The TR of 64HM below a pitch factor of 1.0 was almost equal to the gantry rotation time, while a pitch factor of >1.0 resulted in TR being approximately one half of the gantry rotation time. This property indicated that the reconstruction algorithm of 64HM changes over a partial scan reconstruction algorithm at a pitch factor of 1.0. Hence, to adjust the TR for various projection data for 64HM, we deduced that a weighting function that regulates the range of required projection data to the z-direction based on a modified reconstruction algorithm of a helical filter interpolation and a helical half-scanning was used [2].

The influence of the TRs on image quality for the 128-slice DSCT scanner and the 320-row ADCT scanner using a moving rod phantom is shown in Fig. 4. A rod phantom with a 15-mm diameter was placed at along the perpendicular axis to the gantry rotation plane and moved along the y-axis during helical scanning with a constant speed of 9.5 mm/s (Fig. 4a). These images clearly show perceptual differences of the rod under the same acquisition conditions, in which a lower TR value negatively influenced the shape reproducibility of the moving rod phantom (Fig. 4b). Generally, since the specific reconstruction algorithm of a modern CT scanner is a black-box, detailed comparison of these trajectories is difficult. However, these trajectories along the y-axis of 128-slice DSCT in helical acquisition mode were narrowed with a larger pitch factor, but the 320-row ADCT did not continuously change, as observed with the rod trajectory of DSCT. We suspect that these rod trajectories indicate the individual TR properties in the helical acquisition mode.

Recently, several papers have reported that the thoracic aorta motion artefact for computed tomography angiography of the whole aorta can be reduced by a high pitch mode (DHM) with 128-slice DSCT and an electrocardiogram-gated CT acquisition mode [17-19]. However, these special acquisition modes to reduce the motion artefacts are not necessarily available in all CT scanners. Our TR results indicated that the

change in pitch factor of 1.5 from 0.5 for the 320-row ADCT and the 128-slice DSCT yields an improvement in the TR value of 50% and 72%, respectively. We strongly feel that radiologists should choose a reasonable acquisition mode for the individual CT scanner for difficult patients, such as those with acute or chronic aortic dissection, restless patients (e.g., children), and patients who cannot hold their breath for the long required time. Furthermore, slow CT scanning [5, 20, 21] is an uncomplicated method to achieve a relatively good estimate of the internal target volume for treatment planning, which involves using a slow gantry rotation speed (lower TR) to capture the tumor motion effect under free breathing during each slice acquisition. The minimum TR value indicates that the SHM is poorer than the nominal gantry rotation time and the minimum TR value of the 64HM is almost equal to the gantry rotation time. Therefore, the TR property in the helical acquisition mode, as with a 128-slice DSCT scanner, may adapt to a slow CT scan under free breathing by using a combination of the longest gantry rotation time and the lowest pitch factor. Thus, the result of the TR analysis may be related to setting of appropriate acquisition conditions for several clinical applications. However, because the present study aimed to analyse the TR (FWHM) of the TSP, these result may not sufficiently reflect the overall temporal element in CT images. Therefore, although the detailed relation between the TSP shape and image quality has to be considered as a function of temporal modulation transfer, which was calculated by Fourier transformation of the TSP [11], characterization of the temporal property of the TSP was partly possible using the index of FWHM in our TR measurement.

In conclusion, remarkable differences in the TR property of the helical acquisition modes between the 128-slice DSCT scanner and 320-row ADCT scanner were confirmed in this study. In addition, our measurement results calculated the maximum TR values of these modern CT scanners. Because the TR of helical acquisition mode is dependent on not only a gantry rotation time but also the pitch factor, an improvement in only a gantry rotation time is not sufficient to effectively reduce the impact of motion artefacts.

References

[1] Fukuda A, Lin PJ, Matsubara K, Miyati T. Measurement of gantry rotation time in modern ct. J Appl Clin Med Phys. 2014;15(1):4517.

[2] Taguchi K, Aradate H. Algorithm for image reconstruction in multi-slice helical CT. Med Phys 1998;25(4):550-61.

[3] Hu H. Multi-slice helical CT: scan and reconstruction. Med Phys 1999;26(1): 5-18.

[4] Schaller S, Flohr T, Klingenbeck K, Krause J, Fuchs T, Kalender WA. Spiral interpolation algorithm for multislice spiral CT--part I: theory. IEEE Trans Med Imaging. 2000;19(9):822-34.

[5] Chinneck CD, McJury M, Hounsell AR. The potential for undertaking slow CT using a modern CT scanner. Br J Radiol. 2010;83(992):687-93.

[6] Toshiba Aquilion ONE operation manual. Toshiba Medical Systems, Tokyo, Japan: 2008.

[7] SOMATOM Definition Flash System Owner Manual. Siemens AG, Healthcare Sector; Forchheim, Germany: 2009.

[8] Taguchi K, Anno H. High temporal resolution for multislice helical computed tomography. Med Phys. 2000;27(5):861-72.

[9] Polacin A, Kalender WA, Marchal G. Evaluation of section sensitivity profiles and image noise in spiral CT. Radiology. 1992;185(1):29-35.

[10] Polacin A, Kalender WA, Brink J, Vannier MA. Measurement of slice sensitivity profiles in spiral CT. Med Phys. 1994;21(1):133-40.

[11] Ichikawa K, Hara T, Urikura A, Takata T, Ohashi K. Assessment of temporal resolution of multi-detector row computed tomography in helical acquisition mode using the impulse method. Phys Med. 2015;31(4):374-81.

[12] Flohr TG, Leng S, Yu L, Aiimendinger T, Bruder H, Petersilka M, et al. Dual-source spiral CT with pitch up to 3.2 and 75 ms temporal resolution: image reconstruction and assessment of image quality. Med Phys. 2009;36(12):5641-53.

[13] Endo M, Mori S, Kandatsu S, Tanada S, Kondo C. Development and performance evaluation of the second model 256-detector row CT. Radiol Phys Technol. 2008;1(1):20-6.

[14] Rasband, W.S., ImageJ, U. S. National Institutes of Health, Bethesda, Maryland, USA, http://imagej.nih.gov/ij/, 1997-2015.

[15] Ertel D, Kröber E, Kyriakou Y, Langner O, Kalender WA. Modulation transfer function-based assessment of temporal resolution: validation for single- and dual-source CT. Radiology. 2008;248(3):1013-7.

[16] McCollough CH, Schmidt B, Yu L, Primak A, Ulzheimer S, Bruder H, et al. Measurement of temporal resolution in dual source CT. Med

Phys. 2008;35(2):764-8.
[17] Roos JE, Willmann JK, Weishaupt D, Lachat M, Marincek B, Hilfiker PR. Thoracic aorta: motion artifact reduction with retrospective and prospective electrocardiography-assisted multi-detector row CT. Radiology. 2002;222(1):271-7.
[18] Li Y, Fan Z, Xu L, Yang L, Xin H, Zhang N, et al. Prospective ECG-gated 320-row CT angiography of the whole aorta and coronary arteries. Eur Radiol. 2012;22(11):2432-40.
[19] Nakagawa J, Tasaki O, Watanabe Y, Azuma T, Ohnishi M, Ukai I, et al. Reduction of thoracic aorta motion artifact with high-pitch 128-slice dual-source computed tomographic angiography: a historical control study. J Comput Assist Tomogr. 2013;37(5):755-9.
[20] Wurstbauer K, Deutschmann H, Kopp P, Sedlmayer F. Radiotherapy planning for lung cancer: slow CTs allow the drawing of tighter margins. Radiother Oncol. 2005;75(2):165-70.
[21] Keall PJ, Mageras GS, Balter JM, Emery RS, Forster KM, Jiang SB, et al. The management of respiratory motion in radiation oncology report of AAPM Task Group 76. Med Phys. 2006;33(10):3874-900.

Figure legends

Figure 1. (a) Photograph of the launching platform for TR measurement. (b) Impulse response images of respective CT scanners: (left) SHM for DSCT, (middle) DHM for DSCT; (right) 64HM and 160HM for ADCT. The black arrow in the photograph indicates the flying direction of the small metal ball.

Figure 2. Measured TSPs for the DSCT and ADCT scanners. (a) SHM and (b) DHM for DSCT. (c) 64HM and (d) 160HM for ADCT. The acquisition conditions are as follows: for SHM, gantry rotation time of 0.5 s and pitch factors of 0.5, 1.0, and 1.5; for DHM, gantry rotation time of 0.285 s and pitch factors of 1.55, 2.5, and 3.2; for 64HM, gantry rotation time of 0.5 s and pitch factors of 0.625, 1.109, and 1.5; for 160HM, gantry rotation time of 0.5 s and pitch factors of 0.569, 0.75, and 0.95. Note: the x-axis scale of (b) DHM is one-fifth of the intervals of the others.

Figure 3. TR results for the DSCT and ADCT scanners as a function of pitch factor and gantry rotation time: (a) SHM and (b) DHM for DSCT; (c) 64HM and (d) 160HM for ADCT. The TR values for DSCT changed proportionally with the pitch factor and gantry rotation time. The lines connecting the data points were estimated using a quadratic polynomial curve-fitting method for SHM and DHM and a least-squares method for 64HM and 160HM.

Figure 4. Perceptual differences of the rod phantom, which moved along the y-axis during the helical scan. (a) Photograph of the experimental set up. (b) Moving rod phantom images: (left row) SHM for DSCT, (right row) 64HM for ADCT. In this motion phantom test, a power injector was utilized as the power source for the motions. The rod images were acquired at 120 kVp; 100 effective mAs; gantry rotation time of 0.5 s; pitch factors of (upper) 0.65, (middle) 0.9, and (bottom) 1.2. The actual TR results of upper, middle, and bottom are as follows: for DSCT, 0.697, 0.490, and 0.307 s; for ADCT, 0.480, 0.475, and 0.242 s. The window settings were: window width (WW) 1000 HU and window level (WL) -500 HU.

Table 1. CT acquisition and reconstruction settings for dual source computed tomography (DSCT) and area detector computed tomography (ADCT)

CT scanner	DSCT		ADCT	
Acquisition mode	SHM	DHM	64HM	160HM
Tube voltage (kVp)	120	120	120	120
Effective mAs	100	100	100	100
Rotation time (s/rot.)	0.285, 0.33, 0.5	0.285	0.275, 0.35, 0.5	0.3, 0.5
Detector configuration (mm)	64 × 0.6	2 × 64 × 0.6	64 × 0.5	160 × 0.5
Pitch factor	0.5, 0.75, 1.0, 1.25, 1.5	1.55, 2.0, 2.5, 3.0, 3.2	0.625, 0.75, 0.85, 0.9, 1.109, 1.2, 1.3, 1.375, 1.4, 1.5	0.596, 0.6, 0.65, 0.75, 0.85, 0.95
Slice thickness (mm)	0.75	0.75	0.5	0.5
Patient table increment (mm)	0.2	0.2	0.2	0.2
Display field of view (mm)	100	100	100	100
Reconstruction kernel	B26	B26	FC01	FC01

SHM: single source helical acquisition mode, DHM: dual source helical acquisition mode, HM: helical acquisition mode.

(a)

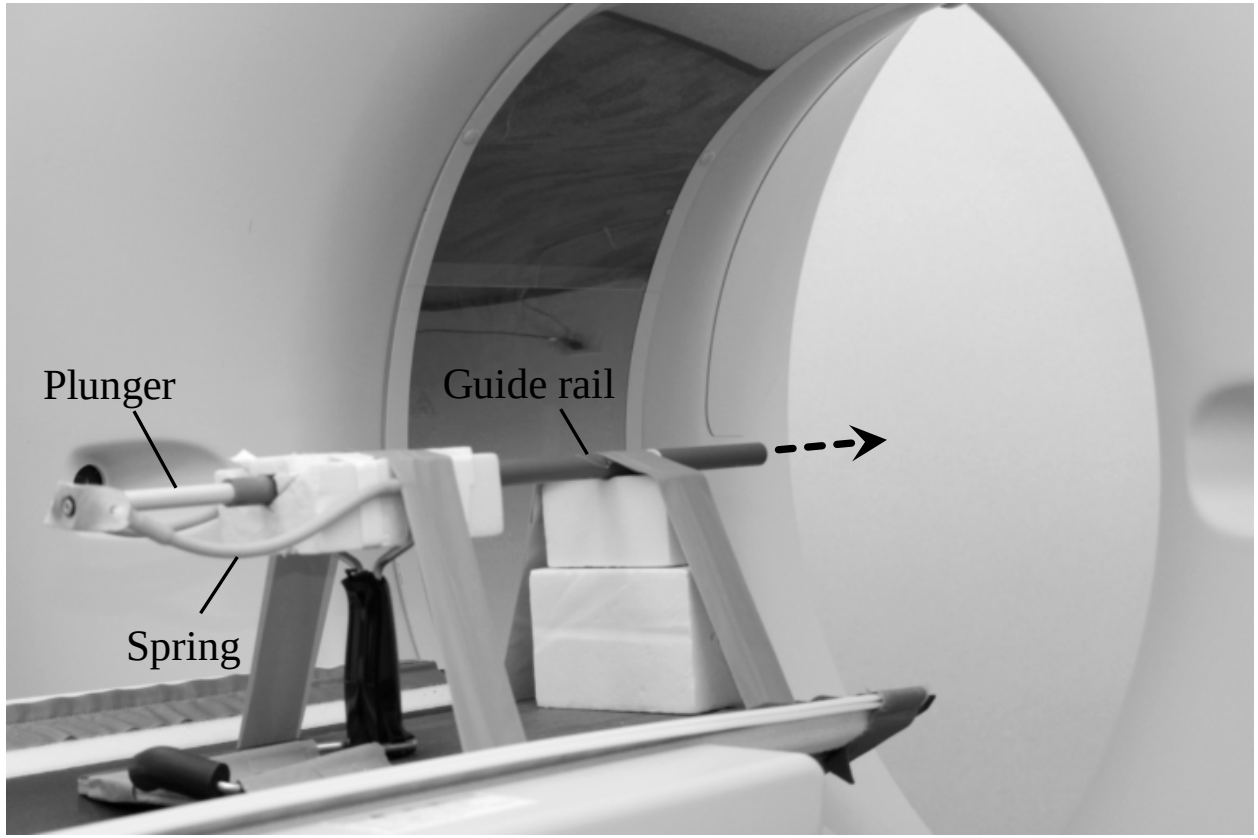

(b)

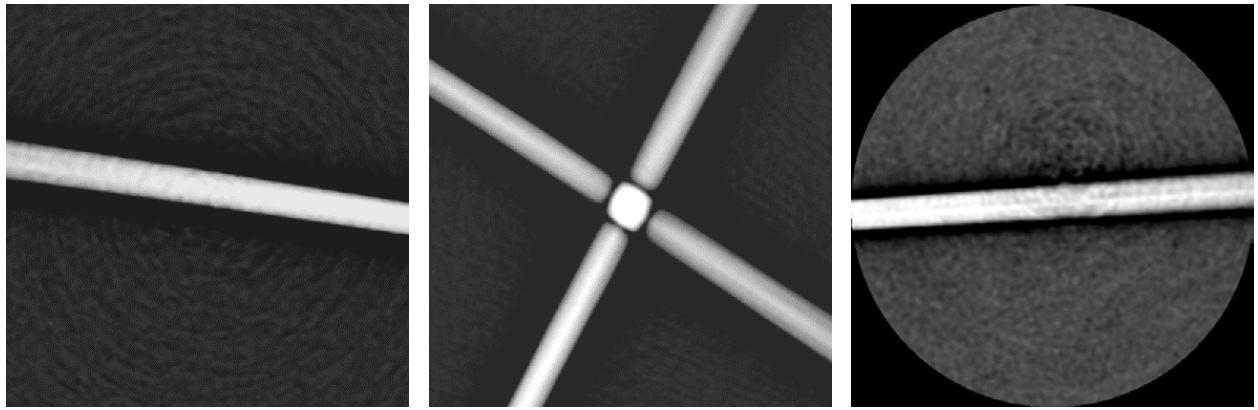

Fig. 1

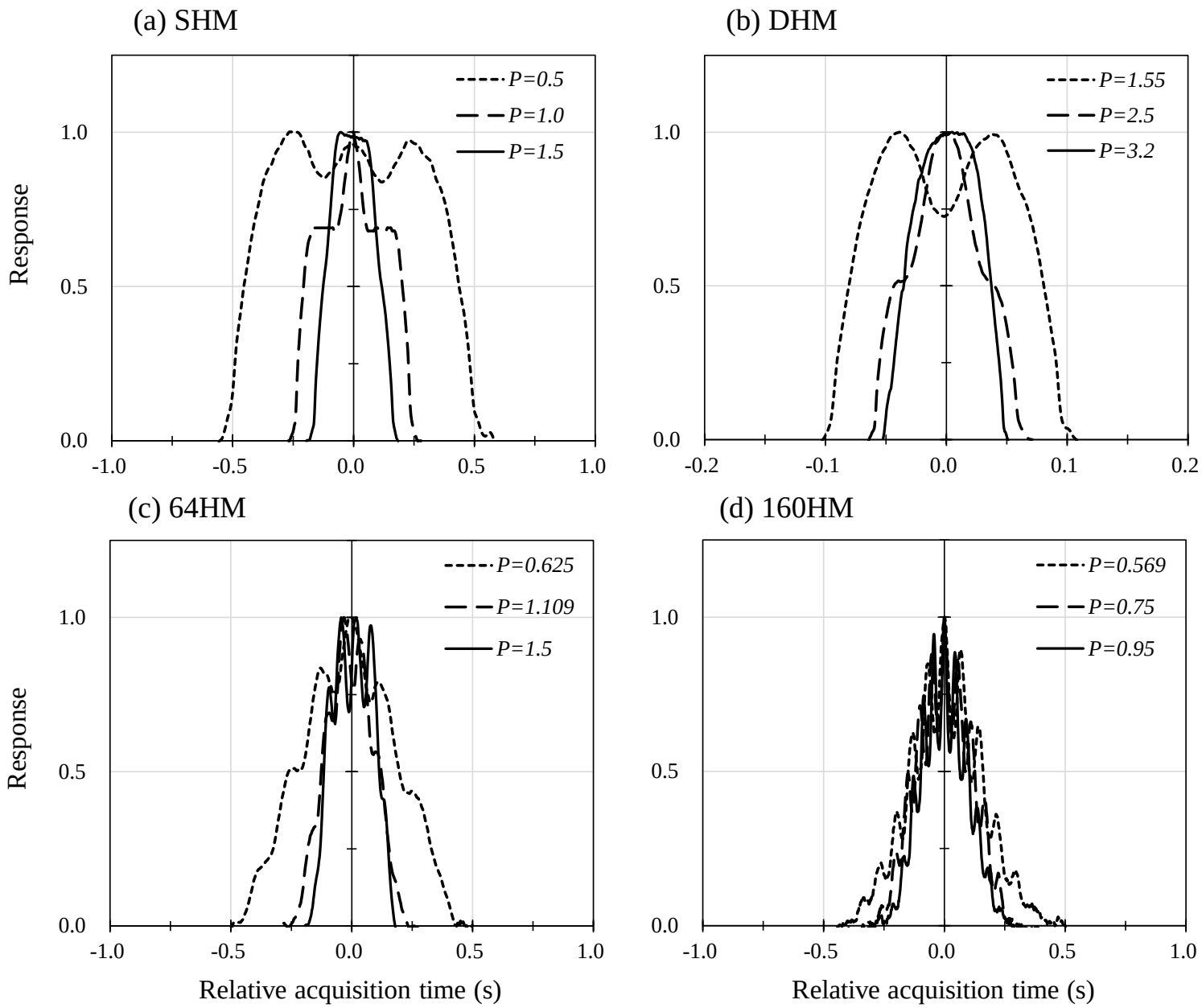
(a) SHM
P=0.5
P=1.0
P=1.5
Response
1.0
0.5
0.0
-1.0
-0.5
0.0
0.5
1.0
(b) DHM
P=1.55
P=2.5
P=3.2
1.0
0.5
0.0
-0.2
-0.1
0.0
0.1
0.2
(c) 64HM
P=0.625
P=1.109
P=1.5
Response
1.0
0.5
0.0
-1.0
-0.5
0.0
0.5
1.0
Relative acquisition time (s)
(d) 160HM
P=0.569
P=0.75
P=0.95
1.0
0.5
0.0
-1.0
-0.5
0.0
0.5
1.0
Relative acquisition time (s)

Fig. 2

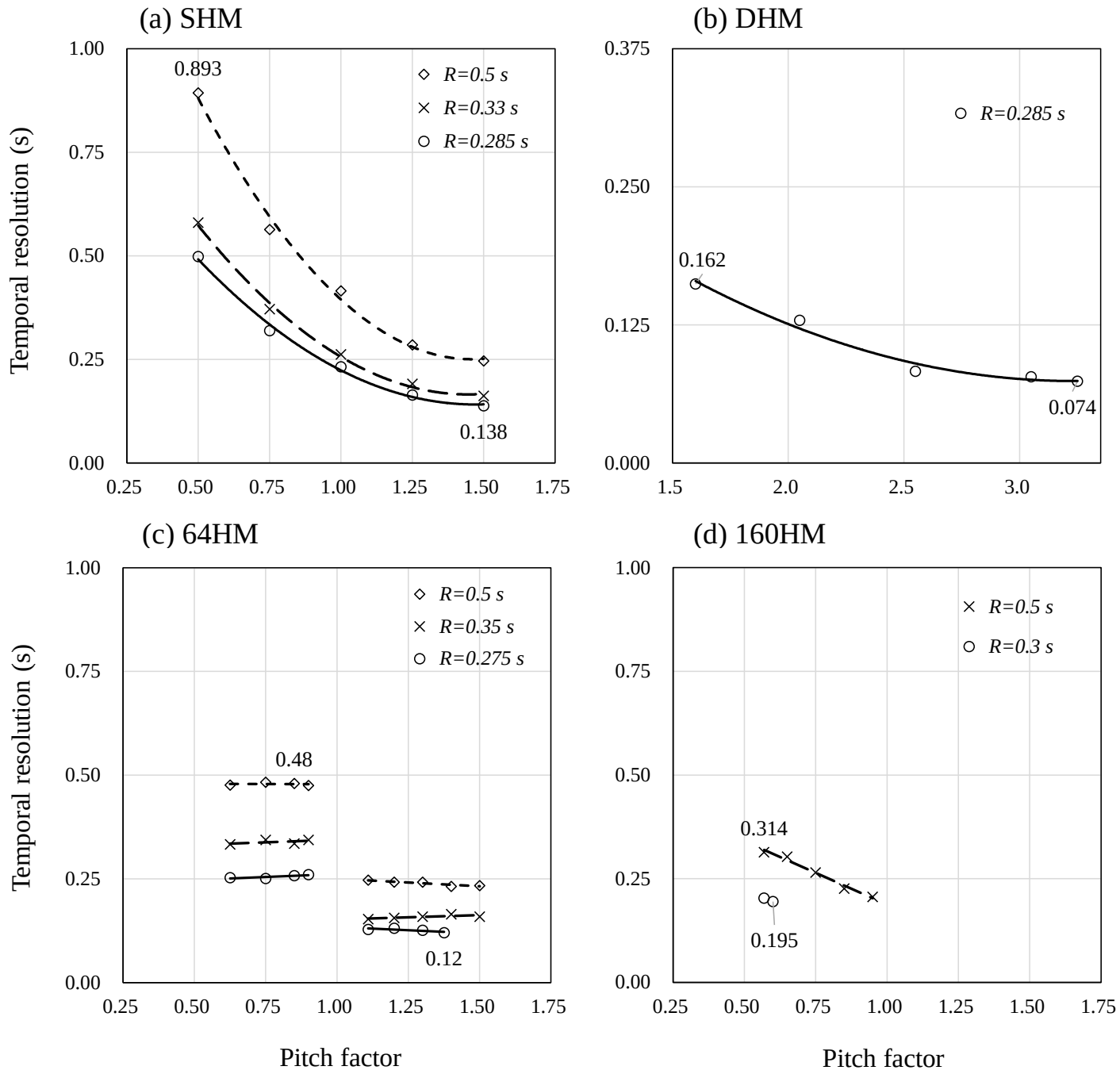
(a) SHM
(b) DHM
(c) 64HM
(d) 160HM
Temporal resolution (s)
Pitch factor
R=0.5 s
R=0.33 s
R=0.285 s
R=0.35 s
R=0.275 s
R=0.3 s
0.893
0.138
0.162
0.074
0.48
0.12
0.314
0.195

Fig. 3

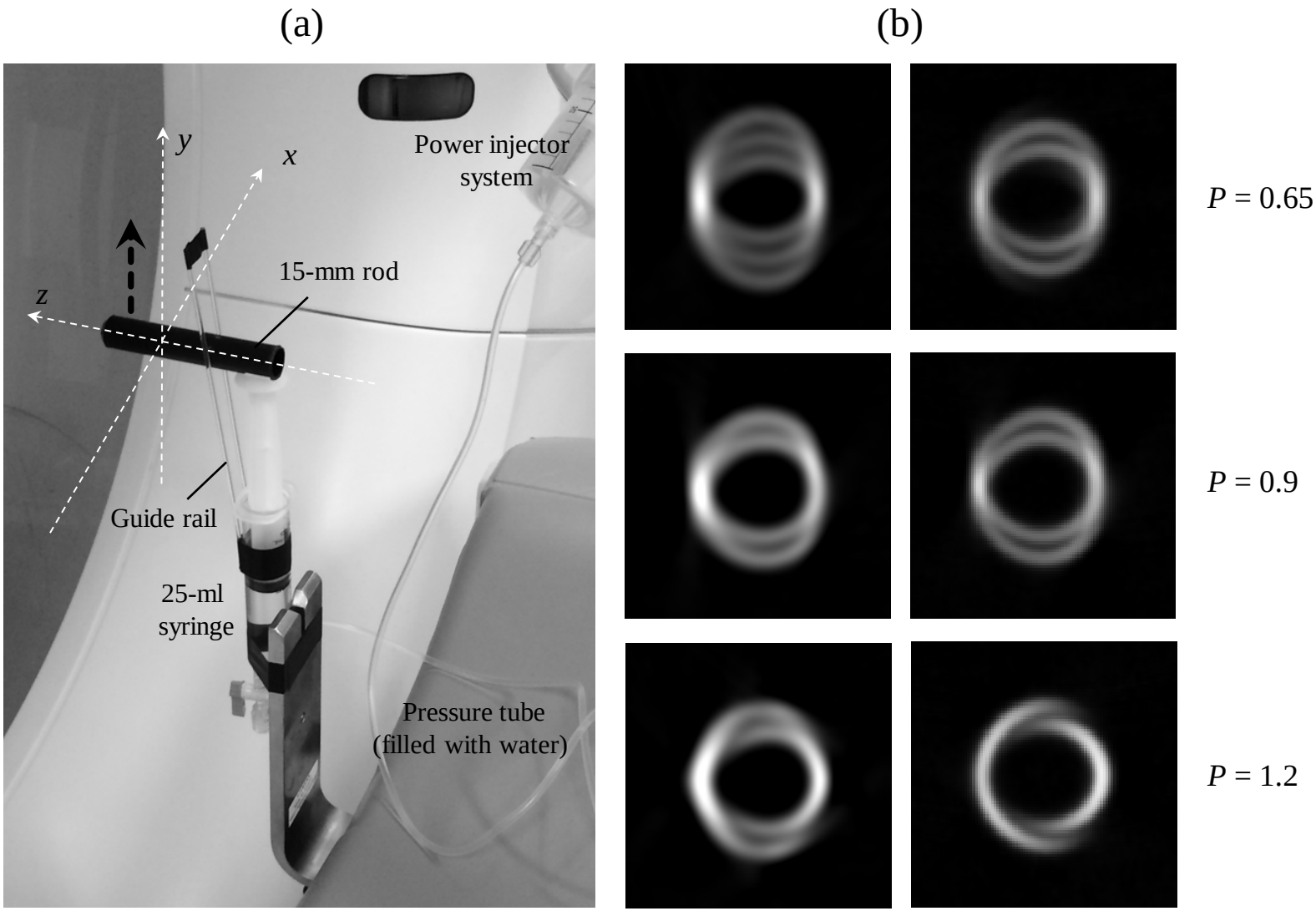
(a)
(b)
y
x
z
Power injector system
15-mm rod
Guide rail
25-ml syringe
Pressure tube (filled with water)
P = 0.65
P = 0.9
P = 1.2

Fig. 4